

# Radiocarbon Measurements Reveal Underestimated Fossil CH<sub>4</sub> and CO<sub>2</sub> Emissions in London

**Journal Article****Author(s):**

Zazzeri, Giulia; Graven, Heather; Xu, Xiaomei; Saboya, Eric; Blyth, Liam; Manning, Alistair J.; Chawner, Hannah; Wu, Dien; Hammer, Samuel

**Publication date:**

2023-08-16

**Permanent link:**

<https://doi.org/10.3929/ethz-b-000625513>

**Rights / license:**

[Creative Commons Attribution-NonCommercial 4.0 International](#)

**Originally published in:**

Geophysical Research Letters 50(15), <https://doi.org/10.1029/2023GL103834>

# Geophysical Research Letters<sup>®</sup>



## RESEARCH LETTER

10.1029/2023GL103834

### Key Points:

- Atmospheric radiocarbon measurements in central London reveal higher fossil CH<sub>4</sub> and CO<sub>2</sub> present, compared to simulations
- Radiocarbon measurements show biospheric uptake of CO<sub>2</sub> in July that is stronger than simulations
- Nuclear power plants interfere with radiocarbon measurements in London when air is coming from Europe

### Supporting Information:

Supporting Information may be found in the online version of this article.

### Correspondence to:

G. Zazzeri,  
gzazzeri@phys.ethz.ch

### Citation:

Zazzeri, G., Graven, H., Xu, X., Saboya, E., Blyth, L., Manning, A. J., et al. (2023). Radiocarbon measurements reveal underestimated fossil CH<sub>4</sub> and CO<sub>2</sub> emissions in London. *Geophysical Research Letters*, 50, e2023GL103834. <https://doi.org/10.1029/2023GL103834>

Received 28 MAR 2023

Accepted 16 JUL 2023

### Author Contributions:

**Conceptualization:** Giulia Zazzeri, Heather Graven

**Data curation:** Giulia Zazzeri, Xiaomei Xu, Eric Saboya, Liam Blyth, Alistair J. Manning, Hannah Chawner, Dien Wu, Samuel Hammer

**Funding acquisition:** Heather Graven

**Investigation:** Giulia Zazzeri

**Methodology:** Giulia Zazzeri, Eric Saboya, Liam Blyth, Alistair J. Manning

**Project Administration:** Heather Graven

**Supervision:** Heather Graven

**Validation:** Heather Graven, Xiaomei Xu

**Writing – original draft:** Giulia Zazzeri

**Writing – review & editing:** Giulia Zazzeri

© 2023 The Authors.

This is an open access article under the terms of the [Creative Commons Attribution-NonCommercial License](#), which permits use, distribution and reproduction in any medium, provided the original work is properly cited and is not used for commercial purposes.

## Radiocarbon Measurements Reveal Underestimated Fossil CH<sub>4</sub> and CO<sub>2</sub> Emissions in London

Giulia Zazzeri<sup>1,2</sup> , Heather Graven<sup>1</sup> , Xiaomei Xu<sup>3</sup> , Eric Saboya<sup>1,4</sup> , Liam Blyth<sup>1</sup>, Alistair J. Manning<sup>5</sup> , Hannah Chawner<sup>6</sup>, Dien Wu<sup>7</sup>, and Samuel Hammer<sup>8</sup>

<sup>1</sup>Physics Department, Imperial College, London, UK, <sup>2</sup>Now at Physics Department, ETH Zurich, Zürich, Switzerland, <sup>3</sup>Earth System Science, University of California Irvine, Irvine, CA, USA, <sup>4</sup>Now at School of Geographical Sciences, Bristol, UK, <sup>5</sup>Met Office, Exeter, UK, <sup>6</sup>School of Chemistry, Bristol, UK, <sup>7</sup>Division of Geological and Planetary Sciences, California Institute of Technology, Pasadena, TX, USA, <sup>8</sup>Institute of Environmental Physics, Heidelberg University, ICOS-CRL, Heidelberg, Germany

**Abstract** Radiocarbon (<sup>14</sup>C) is a powerful tracer of fossil emissions because fossil fuels are entirely depleted in <sup>14</sup>C, but observations of <sup>14</sup>CO<sub>2</sub> and especially <sup>14</sup>CH<sub>4</sub> in urban regions are sparse. We present the first observations of <sup>14</sup>C in both methane (CH<sub>4</sub>) and carbon dioxide (CO<sub>2</sub>) in an urban area (London) using a recently developed sampling system. We find that the fossil fraction of CH<sub>4</sub> and the atmospheric concentration of fossil CO<sub>2</sub> are consistently higher than simulated values using the atmospheric dispersion model NAME coupled with emission inventories. Observed net biospheric uptake in June–July is not well correlated with simulations using the SMURF model with NAME. The results show the partitioning of fossil and biospheric CO<sub>2</sub> and CH<sub>4</sub> in cities can be evaluated and improved with <sup>14</sup>C observations when the nuclear power plants influence is negligible.

**Plain Language Summary** Radiocarbon (<sup>14</sup>C) is an ideal tracer of fossil emissions, as fossil fuels have lost all <sup>14</sup>C during millions of years of burial underground. When fossil carbon is re-introduced into the atmosphere, it exerts a strong dilution of the radiocarbon to total carbon ratio. By measuring this ratio in the atmosphere, we can quantify fossil methane and carbon dioxide emissions. This is the first combined study of <sup>14</sup>C in both atmospheric methane and carbon dioxide at regional scale.

## 1. Introduction

Urban environments hold more than half of the world's population and are responsible for more than 60% of greenhouse gas emissions (World Bank, 2022). Atmospheric measurements of the two major anthropogenic greenhouse gases, CO<sub>2</sub> and CH<sub>4</sub>, in cities have expanded recently and emissions inventories are available at increasingly higher spatial and temporal resolutions (Minx et al., 2021). However, the attribution of emissions to specific source sectors is still largely debated and sectoral emission estimates determined using statistical approaches and associated emission factors are often found to be inconsistent with measurements (Saunois et al., 2020). This is the case of CH<sub>4</sub> emissions in London, where several studies demonstrated that fossil CH<sub>4</sub> emissions are significantly underestimated by emission inventories (Saboya et al., 2022; Zazzeri et al., 2017). CO<sub>2</sub> budgets at urban scale are also difficult to resolve, as processes such as photosynthetic uptake, plant and soil respiration contribute to the net CO<sub>2</sub> exchange and need to be accurately quantified (Miller et al., 2020).

At Imperial College London we have measured radiocarbon (<sup>14</sup>C) in both atmospheric CO<sub>2</sub> and CH<sub>4</sub>. <sup>14</sup>C measurements enable partitioning of the fossil and non-fossil influences on CO<sub>2</sub> and CH<sub>4</sub>. Fossil carbon is completely devoid of <sup>14</sup>C, which has all decayed during millions of years of fossil fuel formation, given a <sup>14</sup>C half-life of 5700 years. When fossil carbon is re-introduced into the atmosphere, it decreases the atmospheric <sup>14</sup>C/C ratio, expressed as Δ<sup>14</sup>C (Stuiver & Polach, 1977), whereas biospheric influences have a much smaller impact on Δ<sup>14</sup>C. By measuring Δ<sup>14</sup>C, we can estimate carbon added from fossil fuels relative to a background site. However these measurements are challenging, especially for atmospheric CH<sub>4</sub>, due to its relatively low concentration (~1.9 ppm) and the large amount of air needed to collect enough carbon for the <sup>14</sup>C analysis via Accelerator Mass Spectrometry (AMS). Another challenge lies in accounting for <sup>14</sup>CH<sub>4</sub> and <sup>14</sup>CO<sub>2</sub> emissions from nuclear power plants (NPPs). In regions where many NPPs are sited, their <sup>14</sup>C emissions can increase the atmospheric Δ<sup>14</sup>C value enough to counteract the fossil carbon dilution (Eisma et al., 1995; Graven & Gruber, 2011).

While  $\Delta^{14}\text{C}$  has been widely used to detect regional fossil  $\text{CO}_2$  emissions (Basu et al., 2020; Graven et al., 2018; Levin, 2008; Wenger et al., 2019), a first quantification of fossil  $\text{CH}_4$  emissions at a regional scale using  $^{14}\text{C}$  in atmospheric  $\text{CH}_4$  has been attempted only for the London region (Zazzeri et al., 2021), finding that the fossil fraction was very high in London, close to 100%. In that study,  $\Delta^{14}\text{CH}_4$  measurements were carried out using a new methodology, which addresses the main sampling challenge of  $\Delta^{14}\text{CH}_4$  measurements by separating carbon during sampling, allowing carbon from hundreds of liters of air to be collected onto a small molecular sieve trap. This method is based on three main steps: (a) trapping of  $\text{H}_2\text{O}$ ,  $\text{CO}_2$  and  $\text{CO}$ , (b) combustion of  $\text{CH}_4$  and (c) adsorption of the  $\text{CH}_4$  combustion-derived  $\text{CO}_2$  into molecular sieves. The trapping method also facilitates collection of  $\text{CO}_2$  samples for  $\Delta^{14}\text{CO}_2$ , enabling high precision  $\Delta^{14}\text{CO}_2$  measurements (Zazzeri et al., 2021).

Here, we build on the previous study by using the same novel technique to collect atmospheric  $\text{CH}_4$  and  $\text{CO}_2$  samples for  $^{14}\text{C}$  analysis between May and July 2020 in London, providing the first combined analysis of fossil  $\text{CH}_4$  and  $\text{CO}_2$  emissions at a regional scale using  $^{14}\text{C}$ . We then compare the observations to model simulations with an emission inventory and biosphere model.

## 2. Materials and Methods

### 2.1. Sampling and $^{14}\text{C}$ Analysis

$\text{CH}_4$  and  $\text{CO}_2$  samples were collected using the sampling system described in Zazzeri et al. (2021). The air was sampled from an air intake on the roof of the Physics department at Imperial College London, at  $\sim 25$  m height. Samples were taken in the afternoon and early evening, when air was well mixed, to avoid sampling of very local emissions and to assess integrated emissions within the London region. Sampling days were chosen based on the availability of the laboratory facilities and on the air provenance. Collection of one  $\text{CH}_4$  sample of  $150 \mu\text{g C}$  took approximately 7 hr, usually from 13:00 to 20:00 (local time).  $\text{CO}_2$  samples of  $\sim 0.5 \text{ mg C}$  were collected at 12:00 over 30 min. A Picarro G2201-i analyzer was used to measure the  $\text{CO}_2$  and  $\text{CH}_4$  mole fractions continuously from the air intake. A detailed description of the setup can be found in Saboya et al. (2022).

Sample traps were sent to the Accelerator Mass Spectrometry facilities in UC Irvine, where  $\text{CO}_2$  was extracted and graphitised for  $^{14}\text{C}$  analysis (Xu et al., 2007).  $\Delta^{14}\text{CH}_4$  measurements are reported with uncertainties of 5–17‰, including background correction for 7 hr of sampling ( $5.5 \pm 0.1 \mu\text{g}$  modern carbon, Zazzeri et al., 2021).  $\Delta^{14}\text{CO}_2$  measurements are reported with uncertainties of 2‰, including background correction ( $1.5 \mu\text{g}$  of modern carbon, Zazzeri et al., 2021).

### 2.2. Quantification of $\text{CH}_4$ Fossil Fraction

The fossil fraction of  $\text{CH}_4$  (i.e., the ratio between fossil and total added  $\text{CH}_4$ ) is calculated following the mass balance approach in Graven et al. (2019). According to this method, fossil emissions will decrease the background atmospheric  $\Delta^{14}\text{CH}_4$  ( $\sim 340$ ‰) by a larger degree than biogenic emissions, due to the different  $^{14}\text{C}$  signatures of fossil ( $-1,000$ ‰) and biogenic  $\text{CH}_4$  sources ( $28 \pm 15$ ‰, based on a turnover time of  $6 \pm 3$  years (Lassey et al., 2007) and the  $\Delta^{14}\text{CO}_2$  record (Graven et al., 2017)). Since  $\Delta^{14}\text{CH}_4$  measurements of background air for 2020 were not available, and the most recent background observations (341‰, Sparrow et al., 2018) date back to 2015, we calculated the fossil fraction of differences in the  $\text{CH}_4$  concentration between pairs of samples collected within 7–11 days with similar air provenance, either from the Atlantic or north of the UK. Thus we assumed that the background air composition was the same for each pair and the influence from NPPs was negligible as there are no NPPs in these directions. We tested the assumption that the influence from NPPs was negligible for these samples with model simulations (Section 2.5).

Three samples were collected when air was coming from Europe, where many pressurized water reactors (PWRs) that emit  $^{14}\text{CH}_4$  (Zazzeri et al., 2018) are sited. These samples showed  $\Delta^{14}\text{CH}_4$  higher than the most recent background value. We did not quantify the fossil fraction for these days, but we simulated the influence of nuclear emissions using a regional atmospheric dispersion model coupled with  $^{14}\text{C}$  emission estimates from NPPs (see Section 2.5).

### 2.3. Quantification of Fossil and Biospheric $\text{CO}_2$

Fossil and biospheric  $\text{CO}_2$  are quantified using mass balances for atmospheric  $\text{CO}_2$  concentrations and  $\Delta^{14}\text{CO}_2$ , following Graven et al., 2018 (Section S1 in Supporting Information S1). We use air samples from Mace Head,

Ireland, collected by the University of Heidelberg cooperative global  $^{14}\text{CO}_2$  background air network and analyzed in cooperation with the Central Radiocarbon Laboratory (CRL) of the Integrated Carbon Observing System (ICOS) to define the  $^{14}\text{CO}_2$  background air composition. Each sample collected in London is compared to the closest in time background sample. We apply corrections for heterotrophic respiration of older carbon with higher  $\Delta^{14}\text{C}$  and for NPP emissions, following Graven et al. (2018) (Section S1 in Supporting Information S1). Sources of NPP  $^{14}\text{CO}_2$  emissions include relatively strong emissions from gas-cooled nuclear reactors in the UK and the reprocessing sites at Sellafield, UK and La Hague, France (Graven & Gruber, 2011), as well as other reactor types present in the UK and Europe. We neglect biomass burning fluxes that are too small to affect our measurements (Crippa et al., 2020). Details on the quantification of NPP and heterotrophic respiration influences are given in Sections 2.4 and 2.5. Biospheric  $\text{CO}_2$  is calculated as the difference between background  $\text{CO}_2$  and fossil  $\text{CO}_2$ , where background  $\text{CO}_2$  concentration is specified for individual days using a model-data technique that combines observations at Mace Head from ICOS with NAME model simulations to identify background conditions at Mace Head, with interpolation and smoothing.

## 2.4. $\text{CO}_2$ and $\text{CH}_4$ Simulations

Model simulations were conducted using the UK Met Office's Numerical Atmospheric-dispersion Modeling Environment (NAME v7.2; Jones et al., 2007). The NAME model produces source-receptor relationships, often referred to as “footprints,” for atmospheric surface measurements—that is, the response of the observations at a measuring station to a source emission. We determined the mole fraction enhancement above background at a particular time by multiplying the footprints with  $\text{CH}_4$  and  $\text{CO}_2$  fluxes provided by the spatially gridded fluxes and integrating over the domain. Footprints were computed for air-histories of 30 days. Footprints used for  $\text{CH}_4$  simulations were time-integrated over the entire 30 days, a domain of  $-25^\circ$ – $25^\circ$  longitude and  $30^\circ$ – $70^\circ$  latitude and resolution of  $0.1^\circ \times 0.1^\circ$ . These footprints, combined with EDGAR emission inventories, produced the best match between simulated  $\text{CH}_4$  concentrations and our  $\text{CH}_4$  observations in London (Saboya et al., 2022). Footprints used for  $\text{CO}_2$  simulations had hourly resolution in the first 24 hr and 29-day integration thereafter, a domain of  $-97.9^\circ$  to  $39.4^\circ$  longitude and  $10.73^\circ$  to  $79.05^\circ$  latitude, and a resolution of  $0.23^\circ \times 0.35^\circ$  (White et al., 2019). Footprints can be found in Section S3 Supporting Information S1.

For  $\text{CH}_4$  fluxes, we used monthly  $\text{CH}_4$  fluxes from EDGARv6. We calculated fossil  $\text{CH}_4$  (sectors: aviation, ship, coal, gas, oil, energy, chemical processes, fossil fuel building, fossil fuel fire) and total  $\text{CH}_4$  enhancements separately and computed a simulated fossil fraction of  $\text{CH}_4$  present. As with the observations, we compared between pairs of simulated  $\text{CH}_4$  corresponding to the observation pairs.

For fossil fuel  $\text{CO}_2$  fluxes, we used monthly fossil fuel emissions from EDGARv4.3 and resolved the monthly emissions into hourly emissions, accounting for the seasonal, weekly and daily variability in  $\text{CO}_2$  emissions based on the UKGHG model (White et al., 2019).

For biospheric  $\text{CO}_2$  fluxes, we used hourly mean net ecosystem exchange (NEE) fluxes from the Solar-Induced Fluorescence for Modeling Urban biogenic Fluxes (“SMUrF”) Model (Wu et al., 2021). For the heterotrophic respiration correction term, heterotrophic respiration fluxes were approximated from the NEE and the mean gross primary production (GPP) fluxes  $([\text{GPP} + \text{NEE}]/2)$  from SMUrF.  $\Delta^{14}\text{C}$  of heterotrophic respiration was assumed to be  $50 \pm 35\text{‰}$  (Section S1 in Supporting Information S1, Graven et al., 2018).

## 2.5. $^{14}\text{C}$ Enhancements From NPPs

The  $^{14}\text{C}$  enhancement due to the emissions from NPPs was also simulated using the NAME footprints. The  $^{14}\text{CO}_2$  and  $^{14}\text{CH}_4$  emissions were specified in two ways: (a) using emission factors based on electrical power production, and (b) with  $^{14}\text{C}$  measurements sourced from the European Commission RADIOACTIVE Discharges Database (RADD 2020).

When using emission factors, we followed the S1 emission factor database in Zazzeri et al., 2018. We attributed two different emission factors to PWRs, based on the reactor model:  $0.407 \pm 0.198 \text{ TBq/GWa}$  for VVER (Russian design) and  $0.193 \pm 0.061 \text{ TBq/GWa}$  for non-VVER reactors. Emission factors were multiplied by 2020 energy outputs retrieved from the International Atomic Energy Agency's Power Reactor Information System (IAEA PRIS 2020). Finally, the  $^{14}\text{C}$  estimates were scaled down by a factor of 53% to represent the  $^{14}\text{CH}_4$  proportion of

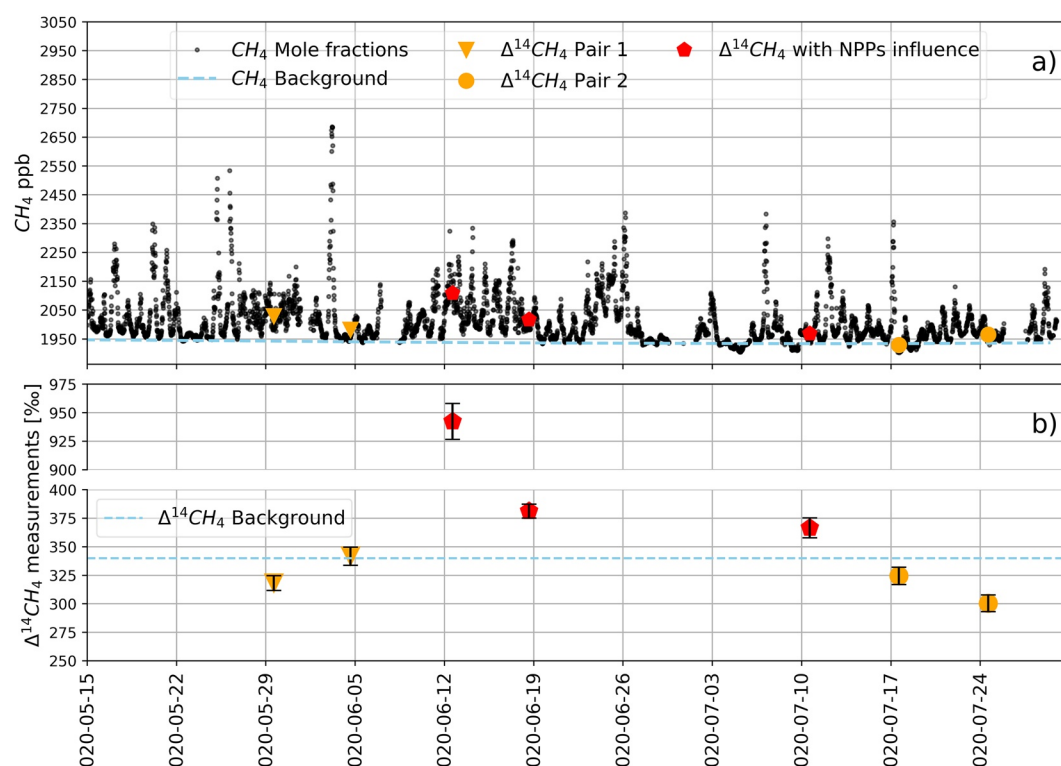


**Figure 1.** (a) Continuous record of 20 min averaged CH<sub>4</sub> mole fraction measurements (black), CH<sub>4</sub> mole fractions of collected samples used for quantification of the fossil fraction (orange), CH<sub>4</sub> mole fraction of samples influenced by <sup>14</sup>CH<sub>4</sub> emissions from NPPs (red), CH<sub>4</sub> mole fraction of background values measured at Mace Head (blue line) and fitted according to Manning et al., 2021. (b) Δ<sup>14</sup>CH<sub>4</sub> values of collected samples using the same color coding, expected background Δ<sup>14</sup>CH<sub>4</sub> of 341‰ based on data from 2015 (Sparrow et al., 2018) (blue line), error bars in black.

total <sup>14</sup>C emissions from PWRs (Kunz, 1985; Zazzeri et al., 2018), and by a factor of 28% for <sup>14</sup>CO<sub>2</sub> emissions from PWRs. We used the Graven and Gruber (2011) emission factors to estimate <sup>14</sup>CO<sub>2</sub> from Gas-cooled reactors (GCRs), advanced Gas-cooled reactors (AGRs) in the UK and Boiling water reactors (BWRs) in Europe, assuming all <sup>14</sup>C emissions to be <sup>14</sup>CO<sub>2</sub>. The <sup>14</sup>CO<sub>2</sub> release from two reprocessing plants, one in the La Hague in France and one in Sellafield in the UK, were retrieved from the RADD database.

### 3. Results

#### 3.1. Δ<sup>14</sup>CH<sub>4</sub> Measurements and Fossil Fraction of CH<sub>4</sub>

Figure 1 shows the continuous record of CH<sub>4</sub> mole fractions measured at Imperial College London over the study period and Δ<sup>14</sup>CH<sub>4</sub> values of the samples collected. The wind direction for the sampling days is shown in Figure S1 in Supporting Information S1. Two sample pairs with measured Δ<sup>14</sup>CH<sub>4</sub> below the expected background level and air provenance from the north or west UK were used for quantification of the CH<sub>4</sub> fossil fraction of the emissions (Table 1). Samples with measured Δ<sup>14</sup>CH<sub>4</sub> above the expected background level were not included.

A fossil fraction (FF) of 99% was calculated from the pair of samples collected when air was coming from the Atlantic, and 69% for one pair collected when air was coming from the north (Table 1). Here the relative fossil fraction is for the CH<sub>4</sub> added between the day with higher CH<sub>4</sub> and the day with lower CH<sub>4</sub>, assuming the 2 days had similar background air composition (same air provenance) and a negligible NPP influence (see Table S1 in Supporting Information S1). Estimated background CH<sub>4</sub> concentrations at the Mace Head station were also comparable for each pair.

The simulated FF for the CH<sub>4</sub> difference between the pairs of samples is smaller than the measured FF, suggesting that the EDGAR v6 inventory coupled with the NAME model may underestimate fossil CH<sub>4</sub> emissions, similar to the result in Saboya et al., 2022 using δ<sup>13</sup>CH<sub>4</sub> data. The simulated CH<sub>4</sub> mole fraction difference for each pair



**Table 1**

Measured FF of Sample Pairs Collected in London in 2020

Dates	Air provenance	Measured $\Delta\text{CH}_4$ (ppb)	Simulated $\Delta\text{CH}_4$ (ppb)	Measured $\Delta\Delta^{14}\text{C}$ (‰)	Calculated $\text{ffCH}_4$ (ppb)	Measured relative FF (%)	Simulated relative FF (%)
29 May & 4 June	North UK	$47 \pm 3$	59	$24 \pm 10$	$32 \pm 20$	$69 \pm 43$	4
17 & 24 July	Atlantic	$36 \pm 1$	1.2	$24 \pm 10$	$36 \pm 20$	$99 \pm 55$	11

Note. The uncertainty on the FF has been calculated propagating the error on the  $\Delta^{14}\text{C}$  values and mole fraction measurements (Section S5 in Supporting Information S1).

is also not consistent with the measured one, being considerably smaller when air came from the Atlantic but slightly higher when air came from the north. The main source of uncertainty in the fossil fraction is the  $\Delta^{14}\text{CH}_4$  measurement uncertainty, which is in the range of 5–9‰. For future studies, comparison of the observations with representative background air is recommended.

$\Delta^{14}\text{CH}_4$  measurements on 12 June, 18 June and 10 July were higher than the expected background level and NAME simulations indicated they were affected by nuclear power plant emissions (Table S1 in Supporting Information S1). The measurement on 12 June was particularly high ( $942 \pm 17‰$ ). According to the NAME footprints, on 12 June air was coming from Germany, passing through Belgium and then Suffolk, England, where the PWR Sizewell B is located. Sizewell B was offline for a planned outage for a period including 12 June and high emissions are expected during the first weeks of a temporary shut down of the reactor (Lehmuskoski et al., 2021).

### 3.2. $\Delta^{14}\text{CO}_2$ Measurements and Fossil and Biospheric $\text{CO}_2$

$\Delta^{14}\text{CO}_2$  observations in summer 2020 span a range between  $-46.2$  and  $-31.5‰$  (Figure 2), lower than the Mace Head data around  $0‰$ , similar to reported  $\Delta^{14}\text{CO}_2$  depletions in large conurbations such as Los Angeles (Miller et al., 2020). The added  $\text{ffCO}_2$  of samples is between 12 and 20 ppm, whereas the simulated added  $\text{ffCO}_2$  is between 1 and 10 ppm (Table 2).

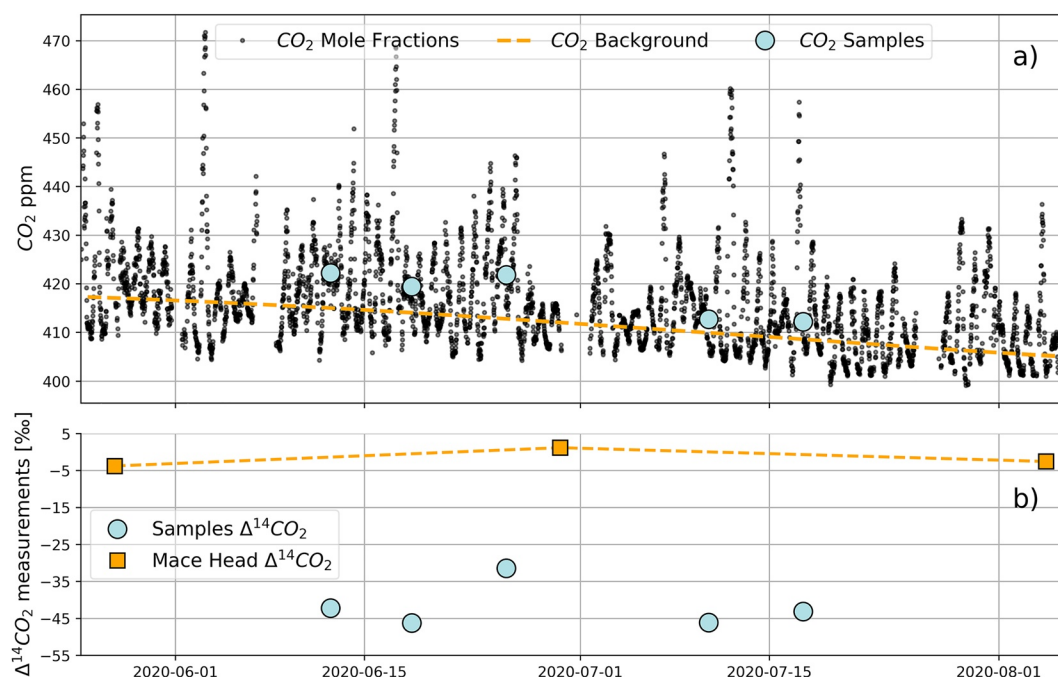


**Figure 2.** (a) Continuous record of 20 min averaged  $\text{CO}_2$  mole fraction measurements (black),  $\text{CO}_2$  mole fractions of collected samples (light blue),  $\text{CO}_2$  mole fraction of background values measured at Mace Head (orange line); (b)  $\Delta^{14}\text{CO}_2$  values of collected samples (light blue).  $\Delta^{14}\text{CO}_2$  of air collected at Mace Head in orange.

**Table 2**

$\Delta^{14}\text{CO}_2$  Measurements of Samples Collected in London in 2020, Calculated and Simulated  $\text{ffCO}_2$  and  $\text{Cveg}$ , and the NPP and Heterotrophic Correction Terms ( $\beta_{\text{NPP}}$  and  $\beta_{\text{HR}}$ )

Date	$\text{CO}_2$ (ppm)	$\Delta^{14}\text{CO}_2$ (‰)	Meas $\text{ffCO}_2$ (ppm)	Sim $\text{ffCO}_2$ (ppm)	Meas $\text{Cveg}$ (ppm)	Sim $\text{Cveg}$ (ppm)	$\beta_{\text{NPP}}$ (ppm)	$\beta_{\text{HR}}$ (ppm)
12/06/2020	$422.2 \pm 2.2$	$-42.3 \pm 1.4$	$17.0 \pm 1.0$	8.6	$-9.8 \pm 1.0$	-14.5	$0.16 \pm 0.05$	$0.57 \pm 0.4$
18/06/2020	$419.4 \pm 2.0$	$-46.3 \pm 1.8$	$19.4 \pm 1.1$	9.6	$-14.0 \pm 1.1$	-24.0	$0.83 \pm 0.31$	$0.57 \pm 0.4$
25/06/2020	$421.8 \pm 0.5$	$-31.5 \pm 2.0$	$12.3 \pm 1.1$	6.6	$-3.3 \pm 1.2$	-8.6	$0.03 \pm 0.04$	$0.44 \pm 0.4$
10/07/2020	$412.7 \pm 0.1$	$-46.2 \pm 1.6$	$19.6 \pm 1.0$	1.2	$-16.8 \pm 1.0$	-7.8	$2 \cdot 10^{-5}$	0.06
17/07/2020	$412.2 \pm 0.3$	$-43.2 \pm 1.6$	$18.4 \pm 0.9$	1.4	$-14.8 \pm 1.0$	-6.5	$3 \cdot 10^{-6}$	0.13

*Note.* The uncertainties on  $\text{ffCO}_2$  and  $\text{Cveg}$  have been calculated by propagating the error on the  $\Delta^{14}\text{C}$  values and mole fraction measurements and the correction terms (Graven et al., 2018).

It is possible that very local emissions, such as  $\text{CO}_2$  emissions from a gas-fired power plant located 200 m east of our inlet, could interfere with our measurements. However, according to Sparks and Toumi (2010), the emission plume from the power station would cross our air inlet only for easterly winds, and with a bigger effect for moderate wind speeds (3–5 m/s). At lower wind speed the plume is going upwards and is not intersecting with our air inlet (see Figure S3 in Supporting Information S1 for the  $\text{CO}_2$  mole fraction record and Table S2 in Supporting Information S1 for the wind data and samples details).

Table 2 includes the applied nuclear ( $\beta_{\text{NPP}}$ ) and the heterotrophic respiration ( $\beta_{\text{HR}}$ ) correction terms on the final fossil  $\text{CO}_2$  mole fraction ( $\text{ffCO}_2$ ) expressed as ppm of  $\text{ffCO}_2$ . The nuclear correction is within the uncertainty of  $\text{ffCO}_2$ . The highest value is on 18 June when air is coming from northern France, where the La Hague reprocessing plant is sited, which, according to the RADD database, releases about 80% of the total  $^{14}\text{C}$  release from NPPs in Europe and the UK. The correction for heterotrophic respiration is within 1 ppm, higher in June.

All samples show a negative biospheric  $\text{CO}_2$  contribution ( $\text{Cveg}$  in Table 2), indicating that the biosphere acts as a net sink, taking up from 3 to 17 ppm. The simulated biospheric contribution is also negative, but there are significant differences in the magnitude of  $\text{Cveg}$  between the simulations and observations. The  $\text{CO}_2$  uptake is stronger in June in the simulations, partly due to more influence from Europe (Figure S2 in Supporting Information S1), but not in the observations. In the simulations, the London urban region accounts for 15%–44% of the biospheric uptake.

## 4. Discussion and Conclusions

In this work we provide the first source characterization of  $\text{CH}_4$  and  $\text{CO}_2$  using both  $\Delta^{14}\text{CH}_4$  and  $\Delta^{14}\text{CO}_2$  measurements, utilizing a new sampling system (Zazzeri et al., 2021). This study demonstrates the power of  $^{14}\text{C}$  observations to attribute the fossil fuel influence on both  $\text{CO}_2$  and  $\text{CH}_4$ , and that our atmospheric station in central London is well-suited for such measurements as long as sampling days are selected to minimize the influence of nearby nuclear reactors and the La Hague fuel reprocessing site. The chosen sampling period is representative of summer conditions in London. A future comparison with samples collected in other seasons is needed for a better understanding of  $\text{CH}_4$  and  $\text{CO}_2$  emissions within the city.

The fossil fraction of added  $\text{CH}_4$  was very high for the sample pairs with air provenance from the Atlantic or north of the UK that had no NPP influence. Simulated fossil fractions of added  $\text{CH}_4$  between the samples in each pair were much lower, demonstrating that the EDGARv6 emissions inventory is likely to underestimate fossil  $\text{CH}_4$  in the London region, similar to prior studies finding underestimated natural gas emissions in London (Helfter et al., 2016; Saboya et al., 2022; Zazzeri et al., 2017). However, the uncertainty on the calculated  $\text{CH}_4$  fossil fraction is high, from 43% to 55%. Improvements in  $\Delta^{14}\text{CH}_4$  measurements and higher  $\text{CH}_4$  enhancements would improve the fossil fraction uncertainty.

Our  $\Delta^{14}\text{CO}_2$  observations show that during summer in London the biosphere acts as a net sink of  $\text{CO}_2$  that strongly counteracts the influence from fossil fuel emissions. This highlights the importance of tracer measurements such as  $\Delta^{14}\text{CO}_2$  for isolating fossil fuel  $\text{CO}_2$  in urban areas where urban or regional vegetation can

have a significant impact on CO<sub>2</sub> concentrations. As expected, the ffCO<sub>2</sub> concentrations we observed in London (12–20 ppm) are much higher than those observed at a rural site in the UK, which were comparable to the measurement uncertainty (~2 ppm, Wenger et al., 2019). Observations of ffCO<sub>2</sub> using Δ<sup>14</sup>CO<sub>2</sub> in other large urban areas, for example, in Los Angeles, show similar average values on the order of 10 ppm (Graven et al., 2018; Miller et al., 2020). The comparison of observed ffCO<sub>2</sub> and bioCO<sub>2</sub> with simulations in London showed strong discrepancies, where a primary cause is likely to be the low resolution of the NAME atmospheric model, but also potentially low resolution or errors in the fossil fuel and biospheric fluxes in the EDGAR inventory and SMURF model. This study shows how interpretation of in situ or satellite CO<sub>2</sub> measurements in urban areas requires tracer measurements such as Δ<sup>14</sup>CO<sub>2</sub> for quantifying fossil fuel and biospheric CO<sub>2</sub>, as well as high resolution atmospheric modeling and high resolution prior flux maps.

## Data Availability Statement

The data used for this study include the observations at Imperial College London, radiocarbon measurements and simulated values using the Met Office model NAME. They are in a.csv format and available at the following repository: <https://doi.org/10.5281/zenodo.7777987>. Data are accessible to the general public without any restrictions. Figures were made with Matplotlib 3.6.0. (<https://matplotlib.org/>). Maps in the supplementary material were made using Matplotlib with Cartopy (<https://pypi.org/project/Cartopy/>).

## Acknowledgments

This project was funded by the European Research Council (ERC) under the European Union's Horizon 2020 research and innovation programme (grant agreement 67910). NAEI inventories were retrieved from the NAEI website: © Crown 2022 copyright Defra & BEIS via naei.beis.gov.uk, licenced under the Open Government Licence (OGL).

## References

- Basu, S., Lehman, S. J., Miller, J. B., Andrews, A. E., Sweeney, C., Gurney, K. R., et al. (2020). Estimating US fossil fuel CO<sub>2</sub> emissions from measurements of <sup>14</sup>C in atmospheric CO<sub>2</sub>. *Proceedings of the National Academy of Sciences of the USA*, 117(24), 13300–13307. <https://doi.org/10.1073/pnas.1919032117>
- Crippa, M., Solazzo, E., Huang, G., Guizzardi, D., Koffi, E., Muntean, M., et al. (2020). High resolution temporal profiles in the emissions database for global atmospheric research. *Scientific Data*, 7(1), 1–17. <https://doi.org/10.1038/s41597-020-0462-2>
- Eisma, R., Vermeulen, A. T., & Van Der Borg, K. (1995). <sup>14</sup>CH<sub>4</sub> emissions from nuclear power plants in northwestern Europe. *Radiocarbon*, 37(2), 475–483. <https://doi.org/10.1017/s003822200030952>
- Graven, H., Allison, C. E., Etheridge, D. M., Hammer, S., Keeling, R. F., Levin, I., et al. (2017). Compiled records of carbon isotopes in atmospheric CO<sub>2</sub> for historical simulations in CMIP6. *Geoscientific Model Development*, 10(12), 4405–4417. <https://doi.org/10.5194/gmd-10-4405-2017>
- Graven, H., Fischer, M. L., Lueker, T., Jeong, S., Guilderson, T. P., Keeling, R. F., et al. (2018). Assessing fossil fuel CO<sub>2</sub> emissions in California using atmospheric observations and models. *Environmental Research Letters*, 13(6), 065007. <https://doi.org/10.1088/1748-9326/aabd43>
- Graven, H., Hocking, T., & Zazzeri, G. (2019). Detection of fossil and biogenic methane at regional scales using atmospheric radiocarbon. *Earth's Future*, 7(3), 283–299. <https://doi.org/10.1029/2018ef001064>
- Graven, H. D., & Gruber, N. (2011). Continental-scale enrichment of atmospheric <sup>14</sup>CO<sub>2</sub> from the nuclear power industry: Potential impact on the estimation of fossil fuel-derived CO<sub>2</sub>. *Atmospheric Chemistry and Physics*, 11(23), 12339–12349. <https://doi.org/10.5194/acp-11-12339-2011>
- Helfter, C., Tremper, A. H., Hallios, C. H., Kotthaus, S., Björkregren, A., Grimmond, C. S. B., et al. (2016). Spatial and temporal variability of urban fluxes of methane, carbon monoxide and carbon dioxide above London, UK. *Atmospheric Chemistry and Physics*, 16(16), 10543–10557. <https://doi.org/10.5194/acp-16-10543-2016>
- Jones, A., Thomson, D., Hort, M., & Devenish, B. (2007). The UK Met Office's next-generation atmospheric dispersion model, NAME III. In *Air pollution modeling and its application XVII* (pp. 580–589). Springer.
- Kunz, C. (1985). Carbon-14 discharge at three light-water reactors. *Health Physics*, 49(1), 25–35. <https://doi.org/10.1097/00004032-198507000-00002>
- Lasse, K. R., Lowe, D. C., & Smith, A. M. (2007). The atmospheric cycling of radiomethane and the "fossil fraction" of the methane source. *Atmospheric Chemistry and Physics*, 7(8), 2141–2149. <https://doi.org/10.5194/acp-7-2141-2007>
- Lehmuskoski, J., Vasama, H., Hämäläinen, J., Hokkinen, J., Kärkelä, T., Heiskanen, K., et al. (2021). On-line monitoring of radiocarbon emissions in a nuclear facility with cavity ring-down spectroscopy. *Analytical Chemistry*, 93(48), 16096–16104. <https://doi.org/10.1021/acs.analchem.1c03814>
- Levin, I., Hammer, S., Kromer, B., & Meinhardt, F. (2008). Radiocarbon observations in atmospheric CO<sub>2</sub>: Determining fossil fuel CO<sub>2</sub> over Europe using Jungfraujoch observations as background. *Science of the Total Environment*, 391(2–3), 211–216.
- Manning, A. J., Redington, A. L., Say, D., O'Doherty, S., Young, D., Simmonds, P. G., et al. (2021). Evidence of a recent decline in UK emissions of hydrofluorocarbons determined by the InTEM inverse model and atmospheric measurements. *Atmospheric Chemistry and Physics*, 21(16), 12739–12755. <https://doi.org/10.5194/acp-21-12739-2021>
- Miller, J. B., Lehman, S. J., Verhulst, K. R., Miller, C. E., Duren, R. M., Yadav, V., et al. (2020). Large and seasonally varying biospheric CO<sub>2</sub> fluxes in the Los Angeles megacity revealed by atmospheric radiocarbon. *Proceedings of the National Academy of Sciences*, 117(43), 26681–26687. <https://doi.org/10.1073/pnas.2005253117>
- Minx, J. C., Lamb, W. F., Andrew, R. M., Canadell, J. G., Crippa, M., Döbbling, N., et al. (2021). A comprehensive and synthetic dataset for global, regional, and national greenhouse gas emissions by sector 1970–2018 with an extension to 2019. *Earth System Science Data*, 13(11), 5213–5252. <https://doi.org/10.5194/essd-13-5213-2021>
- Saboya, E., Zazzeri, G., Graven, H., Manning, A. J., & Englund Michel, S. (2022). Continuous CH<sub>4</sub> and δ<sup>13</sup>CH<sub>4</sub> measurements in London demonstrate under-reported natural gas leakage. *Atmospheric Chemistry and Physics*, 22(5), 3595–3613. <https://doi.org/10.5194/acp-22-3595-2022>
- Saunio, M., Stavert, A. R., Poulter, B., Bousquet, P., Canadell, J. G., Jackson, R. B., et al. (2020). The global methane budget 2000–2017. *Earth System Science Data*, 12(3), 1561–1623. <https://doi.org/10.5194/essd-12-1561-2020>
- Sparks, N., & Toumi, R. (2010). Remote sampling of a CO<sub>2</sub> point source in an urban setting. *Atmospheric Environment*, 44(39), 5287–5294. <https://doi.org/10.1016/j.atmosenv.2010.07.048>



- Sparrow, K. J., Kessler, J. D., Southon, J. R., Garcia-Tiguerros, F., Schreiner, K. M., Ruppel, C. D., et al. (2018). Limited contribution of ancient methane to surface waters of the US Beaufort Sea shelf. *Science Advances*, 4(1), eaao4842. <https://doi.org/10.1126/sciadv.aao4842>
- Stuiver, M., & Polach, H. A. (1977). Discussion reporting of  $^{14}\text{C}$  data. *Radiocarbon*, 19(3), 355–363. <https://doi.org/10.1017/s0033822200003672>
- Wenger, A., Pugsley, K., O'Doherty, S., Rigby, M., Manning, A. J., Lunt, M. F., & White, E. D. (2019). Atmospheric radiocarbon measurements to quantify  $\text{CO}_2$  emissions in the UK from 2014 to 2015. *Atmospheric Chemistry and Physics*, 19(22), 14057–14070. <https://doi.org/10.5194/acp-19-14057-2019>
- White, E. D., Rigby, M., Lunt, M. F., Smallman, T. L., Comyn-Platt, E., Manning, A. J., et al. (2019). Quantifying the UK's carbon dioxide flux: An atmospheric inverse modelling approach using a regional measurement network. *Atmospheric Chemistry and Physics*, 19(7), 4345–4365. <https://doi.org/10.5194/acp-19-4345-2019>
- World Bank. (2022). Urban development. Retrieved from [www.worldbank.org/en/topic/urbandevelopment/overview](http://www.worldbank.org/en/topic/urbandevelopment/overview)
- Wu, D., Lin, J. C., Duarte, H. F., Yadav, V., Parazoo, N. C., Oda, T., & Kort, E. A. (2021). A model for urban biogenic  $\text{CO}_2$  fluxes: Solar-Induced Fluorescence for Modeling Urban biogenic Fluxes (SMUrF v1). *Geoscientific Model Development*, 14(6), 3633–3661. <https://doi.org/10.5194/gmd-14-3633-2021>
- Xu, X., Trumbore, S. E., Zheng, S., Southon, J. R., McDuffee, K. E., Luttgen, M., & Liu, J. C. (2007). Modifying a sealed tube zinc reduction method for preparation of AMS graphite targets: Reducing background and attaining high precision. *Nuclear Instruments and Methods in Physics Research Section B: Beam Interactions with Materials and Atoms*, 259(1), 320–329. <https://doi.org/10.1016/j.nimb.2007.01.175>
- Zazzeri, G., Lowry, D., Fisher, R. E., France, J. L., Lanoisellé, M., Grimmond, C. S. B., & Nisbet, E. G. (2017). Evaluating methane inventories by isotopic analysis in the London region. *Scientific Reports*, 7(1), 1–13. <https://doi.org/10.1038/s41598-017-04802-6>
- Zazzeri, G., Xu, X., & Graven, H. (2021). Efficient sampling of atmospheric methane for radiocarbon analysis and quantification of fossil methane. *Environmental Science & Technology*, 55(13), 8535–8541. <https://doi.org/10.1021/acs.est.0c03300>
- Zazzeri, G., Yeomans, E. A., & Graven, H. D. (2018). Global and regional emissions of radiocarbon from nuclear power plants from 1972 to 2016. *Radiocarbon*, 60(4), 1067–1081. <https://doi.org/10.1017/rdc.2018.42>

## References From the Supporting Information

- Bozhinova, D., Van Der Molen, M. K., Van Der Velde, I. R., Krol, M. C., Van Der Laan, S., Meijer, H. A. J., & Peters, W. (2014). Simulating the integrated summertime  $\Delta^{14}\text{CO}_2$  signature from anthropogenic emissions over Western Europe. *Atmospheric Chemistry and Physics*, 14(14), 7273–7290. <https://doi.org/10.5194/acp-14-7273-2014>
- Wu, D., Lin, J. C., Oda, T., & Kort, E. A. (2020). Space-based quantification of per capita  $\text{CO}_2$  emissions from cities. *Environmental Research Letters*, 15(3), 035004. <https://doi.org/10.1088/1748-9326/ab68eb>